

# The balance between electronic and steric effects in the template-directed syntheses of [2]catenanes<sup>☆</sup>

Marta Pérez-Alvarez,<sup>a,†</sup> Francisco M. Raymo,<sup>a,‡</sup> Stuart J. Rowan,<sup>a,§</sup> David Schiraldi,<sup>b</sup>  
J. Fraser Stoddart,<sup>a,\*</sup> Zhen-He Wang,<sup>a,||</sup> Andrew J. P. White<sup>c</sup> and David J. Williams<sup>c,\*</sup>

<sup>a</sup>Department of Chemistry and Biochemistry, University of California, Los Angeles, 405 Hilgard Avenue, Los Angeles, CA 90095-1569, USA

<sup>b</sup>KoSa Corporation, P.O. Box 5750, Spartanburg, SC 29307-5750, USA

<sup>c</sup>Department of Chemistry, Imperial College, South Kensington, London SW7 2AY, UK

Received 5 December 2000; accepted 22 January 2001

**Abstract**—Three bis-*p*-phenylene-34-crown-10 (BPP34C10) derivatives bearing ester groups on one or both of their two aromatic rings have been synthesized. These ester-substituted macrocyclic polyethers bind the paraquat dication in solution more strongly than BPP34C10. In contrast, however, acyclic analogs of these macrocyclic polyethers form much weaker complexes with cyclobis(paraquat-*p*-phenylene) (CBPQT<sup>4+</sup>). Likewise, catenane formation is diminished, in parallel with the number and disposition of the ester substituents on the hydroquinone rings of the macrocyclic polyethers. These observations suggest that complex and catenane formation are controlled by opposing recognition features, according to whether the ester-substituted hydroquinone rings assume either a guest or host role in 1:1 complexes with bipyridinium-based species, or lie inside or alongside the CBPQT<sup>4+</sup> component in the [2]catenanes. Steric and electronic factors associated with the ester substituents probably account for the opposing trends in the inter-component recognition behavior. © 2001 Elsevier Science Ltd. All rights reserved.

## 1. Introduction

The challenge to uncover new materials with novel forms and functions is one of the major goals of materials science.<sup>1</sup> Mechanically interlocked molecules,<sup>2</sup> which can be obtained in good yields by self-assembly<sup>3</sup> and template-directed<sup>4</sup> methods, have the potential to produce switches and machines at the molecular level.<sup>5</sup> In addition, these molecules provide a source of mechanical bonds for the construction of macromolecular chains. Indeed, interlocked macromolecules<sup>6</sup> constitute a rapidly expanding field of polymer science. In order to develop a novel synthetic approach to poly[2]catenanes,<sup>6,7</sup> we envisaged the possibility of preparing a series of [2]catenanes<sup>2f,3c,e</sup> incorporating cyclobis(paraquat-*p*-phenylene)<sup>8</sup> interlocked with bis-*p*-

phenylene-34-crown-10 (BPP34C10) derivatives bearing ester substituents on their aromatic rings. Polyesterification of such [2]catenane monomers might be expected to afford a viable synthetic route for the construction of poly[2]catenanes. Here, we report (i) the synthesis of three ester-containing bis-*p*-phenylene-34-crown-10 derivatives, (ii) the synthesis of two related ester-containing acyclic polyethers, (iii) the binding of the macrocyclic polyethers with the paraquat dication, (iv) the complexation of the acyclic polyethers by the cyclobis(paraquat-*p*-phenylene) tetracation, and (v) the template-directed synthesis of three [2]catenanes incorporating the ester-containing macrocycles. The X-ray analyses of (vi) two of the free macrocycles, (vii) two complexes, and (viii) one of the [2]catenanes are also reported. The implications of the findings for the introduction of recognition sites and switching components into polymers are discussed.

<sup>☆</sup> Molecular Meccano, Part 63. For Part 62, see Ref. 18.

**Keywords:** aromatic interactions; catenanes; crystal structures; molecular recognition; template-directed synthesis.

\* Corresponding authors. Tel.: +1-310-206-7078; fax: +1-310-206-1843; e-mail: stoddart@chem.ucla.edu

<sup>†</sup> Present address: Synthetic Processes, Pharma Mar, s.a., C/de la Calera, 28760 Tres Cantos, Madrid, Spain.

<sup>‡</sup> Present address: Department of Chemistry, Center for Supramolecular Science, University of Miami, 1301 Memorial Drive, Coral Gables, FL 33146-0431, USA.

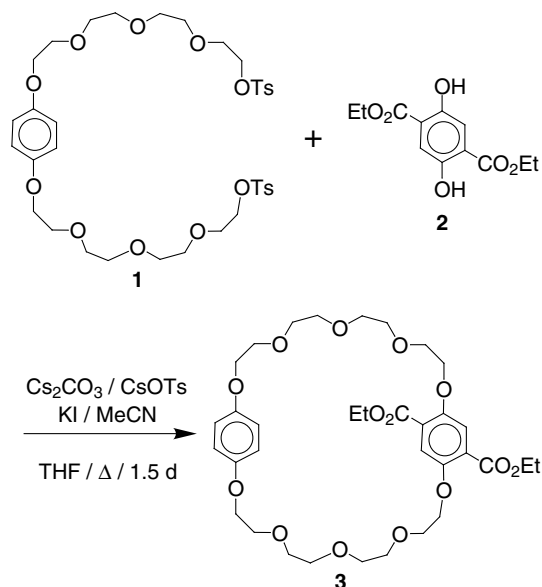
<sup>§</sup> Present address: Department of Macromolecular Science, Case Western Reserve University, 2100 Adelbert Road, OH 44106-7202, USA.

<sup>||</sup> Present address: Department of Chemistry, Virginia Polytechnic Institute and State University, Blacksburg, VA 24061-0212, USA.

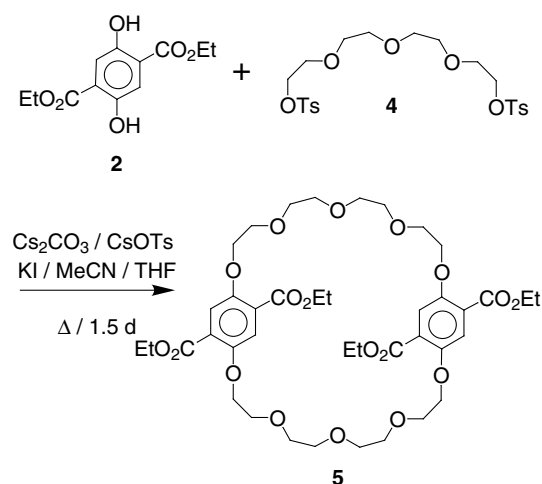
## 2. Results and discussion

### 2.1. Syntheses and binding studies

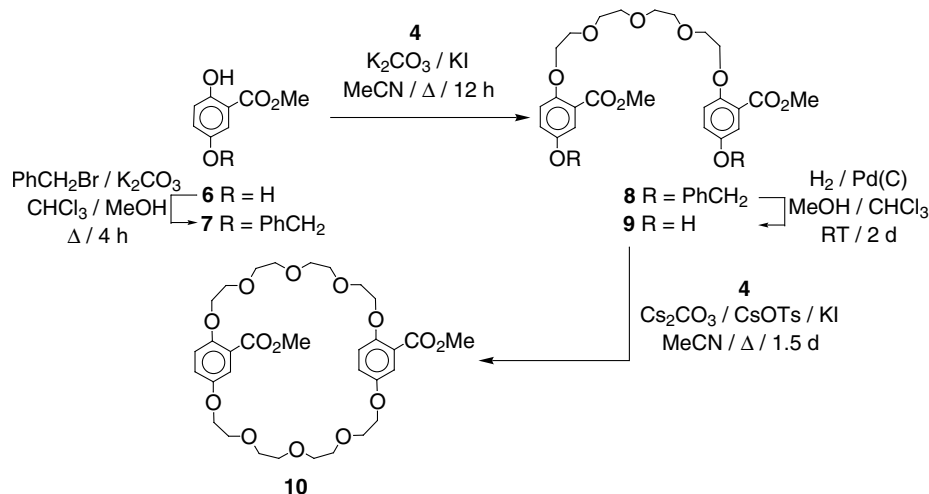
Three BPP34C10 derivatives incorporating ester groups on one or both aromatic rings were prepared following the synthetic routes illustrated in Schemes 1–3. Reaction of the bistosylate **1** with the diol **2** afforded (Scheme 1) the macrocyclic polyether **3**, which incorporates two ester groups *para* to each other on one of its two aromatic



Scheme 1.



Scheme 2.

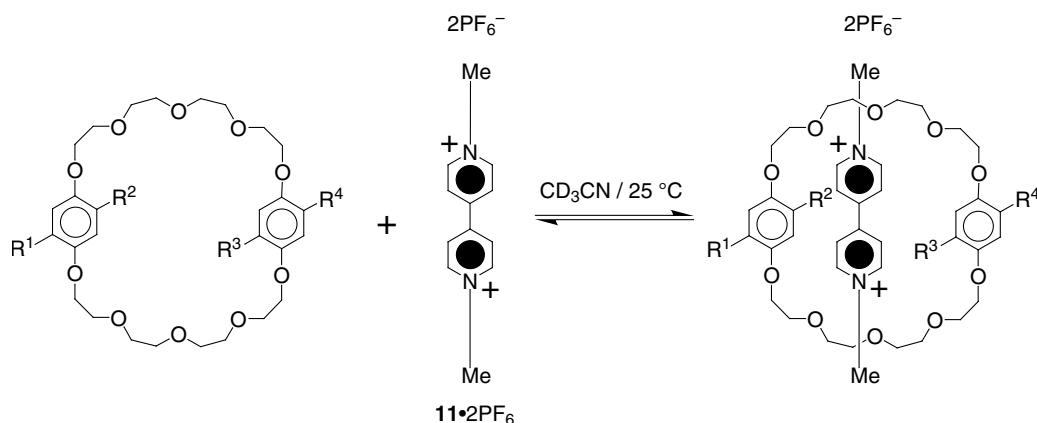


Scheme 3.

rings. Under similar conditions, alkylation of the diol **2** with the bistosylate **4** gave (Scheme 2) the macrocyclic polyether **5**, which has two *para* ester groups on each of its two aromatic rings. Monoprotection of the diol **6**, followed by alkylation with the bistosylate **4**, and then by hydrogenolysis, afforded (Scheme 3) the diol **9**. Reaction of the bistosylate **4** with **9** gave the macrocyclic polyether **10**, which incorporates one ester group on each of its two aromatic rings.

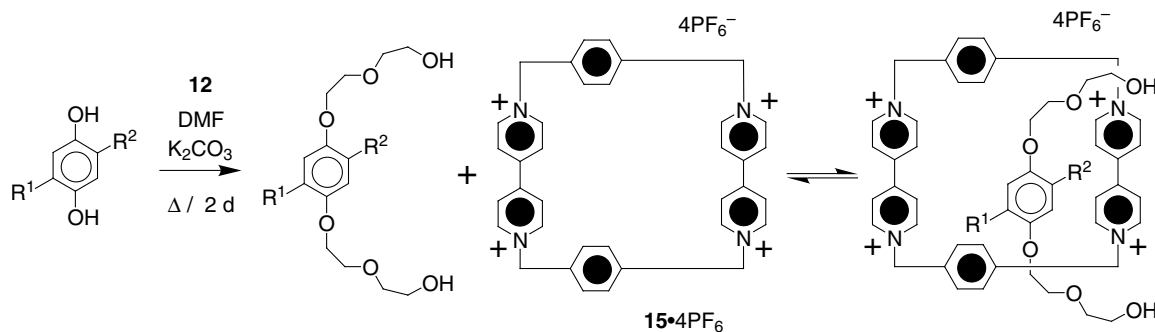
BPP34C10 binds the bipyridinium salt **11**·2PF<sub>6</sub> with a pseudorotaxane geometry, both in solution and in the solid state.<sup>9</sup> The association constant ( $K_a$ ) of the resulting 1:1 complex is 216 M<sup>-1</sup> in CD<sub>3</sub>CN at 25°C. Similar complexes are formed (Scheme 4) when the bipyridinium salt **11**·2PF<sub>6</sub> is mixed with equimolar amounts of **3**, **5**, or **10** in CD<sub>3</sub>CN. The complexes associated with the ester-containing macrocyclic polyethers are, however, more stable than that associated with the parent macrocycle BPP34C10, the  $K_a$  values increasing with the number of ester groups from 291 and 398 M<sup>-1</sup>, respectively, for the macrocyclic polyethers **3** and **10** incorporating two ester groups, to 622 M<sup>-1</sup> for the macrocyclic polyether **5** that has four ester groups. It should be noted that, while the magnitude of the association constant is enhanced with an increase in the number of ester groups on the hydroquinone rings, the colors of the complexes change from reddish-orange for [BPP34C10:**11**]<sub>2</sub>PF<sub>6</sub>, to orange for [**3**:**11**]<sub>2</sub>PF<sub>6</sub>, to yellow for [**5**:**11**]<sub>2</sub>PF<sub>6</sub> and [**10**:**11**]<sub>2</sub>PF<sub>6</sub>, indicating a decrease in the charge transfer component of the interaction.

As a prelude to employing these macrocyclic polyethers as templates for catenane formation, we have synthesized (Scheme 5) acyclic analogs of the ester-containing macrocyclic polyethers by alkylating the diols **2** and **6** with 2-(chloroethoxy)ethanol (**12**). The ability of the resulting polyethers **13** and **14** to thread through the cavity of the bipyridinium-based cyclophane **15**·4PF<sub>6</sub> was explored in CD<sub>3</sub>CN at 25°C. While no complexation was detected for **13**, a  $K_a$  value of 744 M<sup>-1</sup> was determined for the complex formed between **14** and **15**·4PF<sub>6</sub>. However, this complex is significantly less stable than that formed between the same host and the parent guest without ester



|           | R <sup>1</sup>     | R <sup>2</sup>     | R <sup>3</sup>     | R <sup>4</sup>     |                                   |
|-----------|--------------------|--------------------|--------------------|--------------------|-----------------------------------|
| <b>3</b>  | CO <sub>2</sub> Et | CO <sub>2</sub> Et | H                  | H                  | [ <b>3:11</b> ]•2PF <sub>6</sub>  |
| <b>5</b>  | CO <sub>2</sub> Et | CO <sub>2</sub> Et | CO <sub>2</sub> Et | CO <sub>2</sub> Et | [ <b>5:11</b> ]•2PF <sub>6</sub>  |
| <b>10</b> | CO <sub>2</sub> Me | H                  | CO <sub>2</sub> Me | H                  | [ <b>10:11</b> ]•2PF <sub>6</sub> |

Scheme 4.



|          | R <sup>1</sup>     | R <sup>2</sup>     | yield (%)   |                                   |
|----------|--------------------|--------------------|-------------|-----------------------------------|
| <b>2</b> | CO <sub>2</sub> Et | CO <sub>2</sub> Et | <b>13</b> 8 | [ <b>13:15</b> ]•4PF <sub>6</sub> |
| <b>6</b> | H                  | CO <sub>2</sub> Me | <b>14</b> 4 | [ <b>14:15</b> ]•4PF <sub>6</sub> |

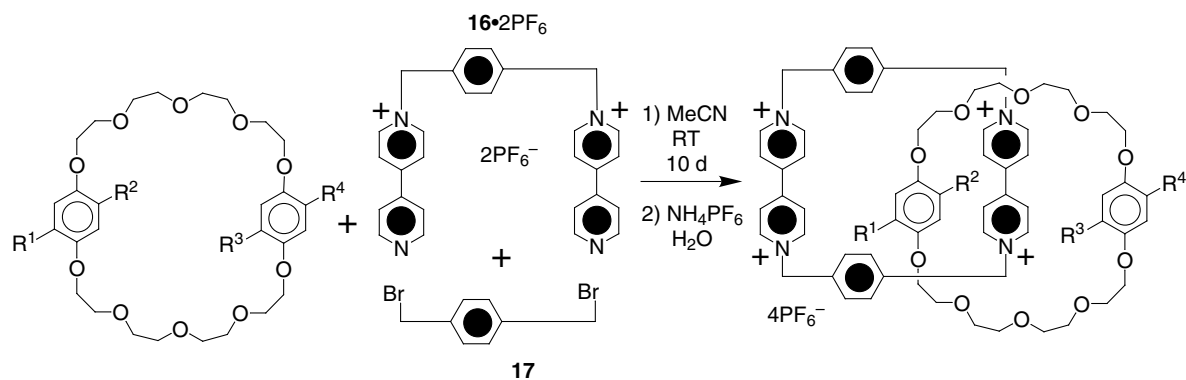
Scheme 5.

substituents (R<sup>1</sup>=R<sup>2</sup>=H in Scheme 5), where the  $K_a$  value is 2220 M<sup>-1</sup>. Thus, the presence of ester groups on the acyclic guest has a detrimental effect on the resulting complex stabilities.

## 2.2. Catenations

The ability of the ester-containing macrocyclic polyethers **3**, **5**, and **10** to template the formation of [2]catenanes, incorporating the bipyridinium-based cyclophane **15**•4PF<sub>6</sub> as their other macrocyclic component, was then explored following the synthetic route shown in Scheme 6. The bis(hexafluorophosphate) salt **16**•2PF<sub>6</sub> was reacted with the dibromide **17** in the presence of **3**, **5**, or **10**. After counterion exchange, the corresponding [2]catenanes **18**•4PF<sub>6</sub>, **19**•4PF<sub>6</sub>, and **20**•4PF<sub>6</sub> were isolated in yields of 53, 3, and 10%, respectively. By contrast, the [2]catenane

incorporating the parent BPP34C10 has been obtained in a yield of 70% under otherwise identical conditions.<sup>10</sup> These observations demonstrate that the yields of the catenations decrease as the number of ester groups increases and that the efficiency of the process is higher when at least one of the two aromatic rings of the macrocyclic polyether does not carry ester substituents, suggesting that these substituents prevent the template-directed formation of the tetracationic cyclophane. The co-conformation adopted (Scheme 6) by the [2]catenane **18**•4PF<sub>6</sub> in CD<sub>3</sub>CN solution is supported by analysis of the chemical shifts for the aromatic protons of the macrocyclic polyether component. The aromatic protons on the disubstituted hydroquinone ring resonate as a singlet at  $\delta$  6.40. The signals for the aromatic protons on the unsubstituted hydroquinone ring overlap with the resonances for the *O*-methylene protons in the range  $\delta$  3.62–3.94. The pronounced up-field shift of these signals demonstrates



|           | R <sup>1</sup>     | R <sup>2</sup>     | R <sup>3</sup>     | R <sup>4</sup>     | yield (%) |                             |
|-----------|--------------------|--------------------|--------------------|--------------------|-----------|-----------------------------|
| <b>3</b>  | H                  | H                  | CO <sub>2</sub> Et | CO <sub>2</sub> Et | 53        | <b>18</b> •4PF <sub>6</sub> |
| <b>5</b>  | CO <sub>2</sub> Et | CO <sub>2</sub> Et | CO <sub>2</sub> Et | CO <sub>2</sub> Et | 3         | <b>19</b> •4PF <sub>6</sub> |
| <b>10</b> | CO <sub>2</sub> Me | H                  | CO <sub>2</sub> Me | H                  | 10        | <b>20</b> •4PF <sub>6</sub> |

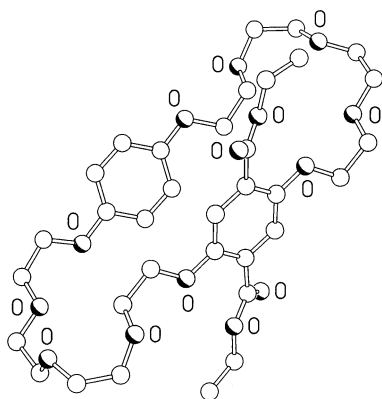
Scheme 6.

that their aromatic ring resides inside the cavity of the tetra-cationic cyclophane as shown in Scheme 6.

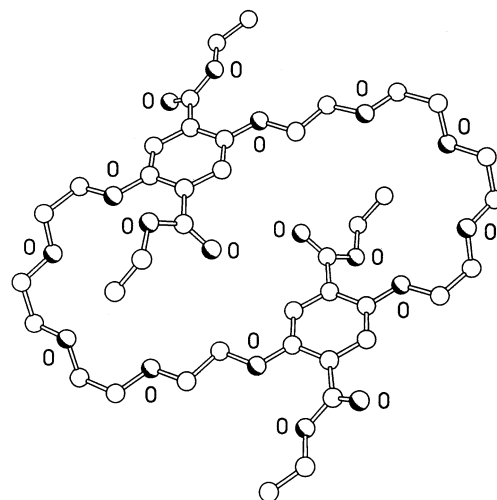
### 2.3. X-Ray crystallography

The macrocyclic polyether **3** is observed (Fig. 1) to be self-filling in the solid state. The two aromatic rings are separated by a ring centroid–ring centroid distance of only 4.48 Å and are mutually inclined by 26°. The two ester groups are rotated by ca. 41 and 33° in opposite directions out of the plane of the aromatic ring. The oxymethylene substituents of each aromatic ring have *anti* and coplanar geometries. The molecules pack to form polar stacks with the 1,4-dioxybenzene ring of one molecule overlying partially the diester substituted aromatic ring of the next. The ring centroid–ring centroid separation is 4.32 Å. There are no interstack interactions of note.

The macrocyclic polyether **5** is seen (Fig. 2) to have a more open and *C<sub>i</sub>* symmetric geometry in the solid state. The two aromatic rings are parallel and separated by a ring centroid–ring centroid distance of 7.20 Å. However, the two aromatic

Figure 1. The solid state structure of the macrocyclic polyether **3**.

rings are inclined at a shallow angle to the plane of the macrocycle and the mean interplanar separation is only 3.89 Å. The ester functions are rotated in the same direction out of the plane of their associated aromatic ring (the torsional angles are ca. 40 and 34° for the ‘inside’ and ‘outside’ ester groups, respectively). The oxymethylene substituents of each aromatic ring have *anti* and coplanar geometries. The polyether loops of **5** accommodate CH<sub>2</sub>Cl<sub>2</sub> molecules held by [C–H···O] hydrogen bonds. However, the solvent molecules are slightly disordered and thus the hydrogen bonding geometries have not been analyzed in detail. Adjacent lattice-translated molecules form off-set stepped stacks. The closest intermolecular separation is between one of the methylene ArOCH<sub>2</sub> hydrogen atoms in one molecule and the aromatic ring of the next and vice versa, though the H–ring centroid distance (3.18 Å) is longer than those normally associated with [C–H···π] interactions.

Figure 2. The solid state structure of the macrocyclic polyether **5**.

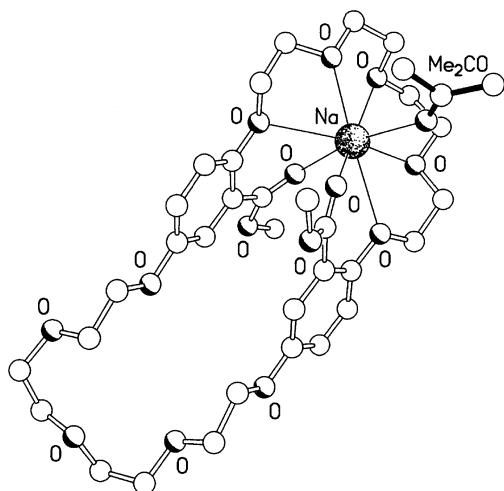


**Figure 3.** Ball-and-stick representation of the geometry adopted by the complex  $[10:Na/Me_2CO]^+$  in the solid state.

In the solid state, the sodium complex  $[10:Na]\cdot PF_6$  of the macrocyclic polyether **10** shows (Fig. 3) the two aromatic rings to be inclined by  $7^\circ$  with a mean interplanar separation of 4.53 Å. The oxymethylene substituents of one aromatic ring have a *syn* geometry, while those of the other adopt an *anti* geometry. The ester groups are rotated out of the plane of their associated aromatic ring (the torsional angles are ca. 24 and  $20^\circ$  for the ‘up’ and ‘down’ ester groups, respectively). The geometries of the two polyether loops are very different. One of them accommodates the  $Na^+$  ion, which interacts with five polyether oxygen atoms {the  $[O\cdots Na^+]$  distances range between 2.508(3) and 2.832(3) Å}, two ester carbonyl oxygen atoms {the  $[O\cdots Na^+]$  distances are 2.344(3) and 2.426(3) Å}, and an oxygen atom of an included  $Me_2CO$  solvent molecule {the  $[O\cdots Na^+]$  distance is 2.539(3) Å}. The complexes pack to form slightly off-set polar stacks with partial overlap of the aromatic rings of lattice-translated molecules (the mean interplanar and ring centroid–ring centroid separations are 3.61 and 4.31 Å, respectively).

In the solid state, the paraquat complex  $[3:11]\cdot 2PF_6$  of the macrocyclic polyether **3** has (Fig. 4) the pyridinium rings of the dication sandwiched between the aromatic rings of the macrocyclic polyether. The mean interplanar separation

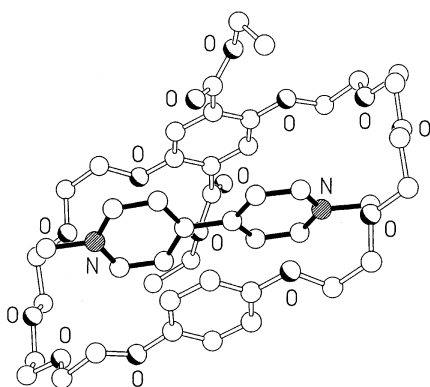


**Figure 4.** Ball-and-stick representation of the geometry adopted by the complex  $[3:11]^{2+}$  in the solid state.

between the ester-substituted aromatic ring and the bipyridinium unit is 3.62 Å, while that between this unit and the other aromatic ring of the host is 3.60 Å. The two aromatic rings of the macrocyclic polyether are not parallel, being inclined by  $9^\circ$ . There is a torsional twist of ca.  $17^\circ$  about the bond linking the two pyridinium rings. Once again, the ester groups are rotated substantially out of the plane of the associated aromatic ring (the torsional angles are ca. 46 and  $56^\circ$  for the ‘up’ and ‘down’ ester groups, respectively). The rotation of the ‘up’ ester group facilitates an intracomplex  $[C-H\cdots O]$  interaction<sup>11</sup> between one of the  $\beta$ -pyridinium hydrogen atoms and the ester carbonyl oxygen atom (interaction (a) in Fig. 5). The complex is stabilized further by  $[C-H\cdots O]$  interactions between the methyl groups of the dicationic paraquat guest and the central oxygen atom of each of the polyether loops—the  $[C\cdots O]$  and  $[H\cdots O]$  distances and  $[C-H\cdots O]$  angle are 3.36, 2.44 Å,  $160^\circ$  and 3.43, 2.48 Å,  $171^\circ$ . Adjacent glide-related complexes are linked by a further  $[C-H\cdots O]$  interaction between the other  $\beta$ -pyridinium hydrogen atoms (on the same pyridinium ring) in one molecule and the other (‘down’) ester carbonyl oxygen atom in the next (interaction (b) in Fig. 5).

The solid state structure (Fig. 6) of the [2]catenane  $20\cdot 4PF_6$  has a geometry reminiscent of the parent [2]catenane<sup>10</sup> wherein one of the ester-substituted hydroquinone rings is sandwiched between the two bipyridinium units of the tetracationic cyclophane with the other lying alongside. The mean interplanar separations between the inside hydroquinone ring and the inside and alongside bipyridinium units are 3.48 and 3.53 Å, respectively. The mean interplanar separation between the alongside ester-substituted hydroquinone ring and the inside bipyridinium unit is 3.50 Å. The ester substituent of the inside hydroquinone ring is oriented almost orthogonally (ca.  $86^\circ$ ) to the plane of its associated ring whereas that of the alongside hydroquinone ring is inclined by ca.  $49^\circ$ . The [2]catenane

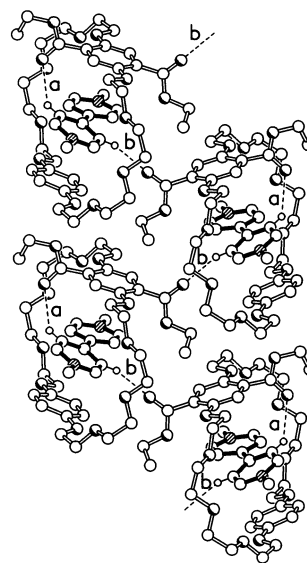


**Figure 5.** Part of one of the  $[C-H\cdots O]$  linked chains of complexes in the structure  $[3:11]\cdot 2PF_6$ . The hydrogen bonding geometries are  $[C\cdots O]$ ,  $[H\cdots O]$  distances (Å),  $[C-H\cdots O]$  angle ( $^\circ$ ) (a) 3.26, 2.49,  $137^\circ$  and (b) 3.19, 2.28,  $157^\circ$ .

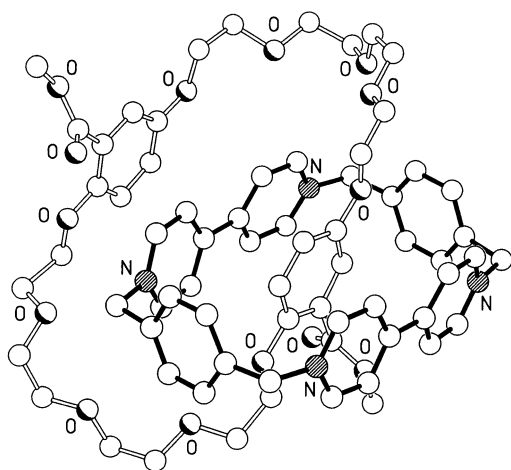


Figure 6. The solid state structure of the [2]catenane  $20^{4+}$ .

molecules pack to form polar stacks with a mean interplanar separation between the alongside ester-substituted hydroquinone ring and the alongside bipyridinium unit of ca. 3.37 Å.

### 3. Conclusions

In summary, BPP34C10 derivatives bearing ester substituents bind the *N,N'*-dimethylbipyridinium dication more strongly than the parent macrocyclic polyether—namely, BPP34C10. The ester groups stabilize the complexes by [C–H···O] interactions between the ester carbonyl oxygen atoms and the bipyridinium hydrogen atoms. These favorable electronic effects are opposed by steric interactions when the ester-containing macrocycles are employed to template the formation of [2]catenanes incorporating cyclobis(paraquat-*p*-phenylene) as their other macrocyclic component. Clipping of the bipyridinium-based cyclophane around a 1,4-dioxybenzene ring bearing ester substituents is impaired by the steric hindrance associated with these groups. Consistently, threading of the preformed cyclobis(paraquat-*p*-phenylene) onto acyclic analogs of the ester-containing macrocycles is also discouraged by the steric hindrance associated with the ester substituents, despite their ability to sustain [C–H···O] interactions. The addition of the electron withdrawing ester groups to the  $\pi$ -electron rich 1,4-dioxybenzene rings leads to competing effects. While the BPP34C10 derivatives carrying ester groups show increased binding of the paraquat dication  $11^{2+}$ , the ester-substituted hydroquinone threads are complexed less strongly by the tetracationic cyclophane  $15^{4+}$ , presumably as a result of unfavorable steric interactions.

The pseudorotaxanes reported in this paper incorporate either a total of four or seven six-membered aromatic rings. The catenanes, on the other hand, contain eight such aromatic rings. While it is known<sup>12</sup> that [C–H···O] interactions are the dominant noncovalent forces stabilizing these systems, the role of the aromatic rings is a critical one. Arene–arene stacking interactions do contribute to pseudorotaxane stabilities and also assist in the formation of the

catenanes. These particular noncovalent interactions are a combination of electrostatic and charge transfer terms. In the ground state, the electrostatic interactions are significantly stronger than the charge transfer ones. They dominate the binding energy associated with the  $[\pi-\pi]$  stacking interactions. The Hunter–Sanders model,<sup>13</sup> which implicates electrostatic interactions arising from out-of-plane  $\pi$ -electron densities, predicts that the maximum  $[\pi-\pi]$  interaction will be observed between two electron-deficient aromatic rings since the repulsion between out-of-plane  $\pi$ -electron densities of such interacting arene units will be minimal. A number of investigations have been carried out on model systems<sup>14</sup> that seem to support this model. This particular theory of arene–arene interactions helps to explain why the electron-deficient ester-containing BPP34C10 derivatives show an increase in binding toward the electron deficient bipyridinium unit in  $11 \cdot 2PF_6$ . The reduction in electron density of 1,4-dioxybenzene rings caused also by their carrying electron-withdrawing ester functions results in a change in the color of the complexes—an observation which indicates a reduced charge-transfer interaction between aromatic units, even though the observed binding increases. It is consistent with previous results,<sup>10</sup> suggesting that the dominant component in arene–arene interactions is  $[\pi-\pi]$  electrostatic and not charge transfer interactions. It should be noted that the increase in the binding of  $11 \cdot 2PF_6$  to the ester-containing BPP34C10 derivatives may also be a consequence of the presence of additional [C–H···O=C] hydrogen bonds such as have been observed (Fig. 5) in the solid-state superstructure of the pseudorotaxane  $[3-11]^{2+}$ .

These pseudorotaxanes and catenanes, which contain electron-poor and electron-rich units also incorporate charge transfer interactions. While considerably weaker than the electrostatic interactions, the charge transfer terms dictate the absorption behavior of these molecules and complexes in the visible region and, as a result, determine their color. This behavior is demonstrated by the changes in color of the paraquat complexes as the hydroquinone units in the crown component become more electron poor upon addition of the ester groups.

The aromatic rings aid the characterization of the threaded complexes and interlocked compounds. We can obtain association constants for the complexes using aromatic ring protons as  $^1H$  NMR probes. Importantly, we have demonstrated that the aromatic units can act as scaffolds onto which useful functional groups can be attached. Although these groups influence the stabilities of complexes and the efficiencies of the catenations as a result of a subtle balance between steric and electronic effects, they provide us with the means to incorporate recognition sites and switches into larger (supra)molecular assemblies, including polymers. The redox active aromatic rings also offer the opportunity of being able to address the complexes and interlocked components with electrochemical stimuli, paving the way for the construction of molecule-based devices.<sup>15</sup> In summary, the various six-membered rings present in these pseudorotaxanes and catenanes determine the (super)structural and physical properties of these novel complexes and compounds.

## 4. Experimental

### 4.1. General methods

Chemicals were purchased from Aldrich and used as received. Solvents were dried according to literature procedures<sup>16</sup> and reactions were carried out under an atmosphere of dry N<sub>2</sub>. The bistosylates **1** and **4** were prepared following published procedures.<sup>10</sup> Thin layer chromatography (TLC) was carried out on aluminum sheets coated with SiO<sub>2</sub> 60 (Merck 5554). Column chromatography was performed on SiO<sub>2</sub> 60 (Merck 9385, 230–400 mesh). Melting points were determined on an Electrothermal 9200 apparatus and are uncorrected. Electron impact mass spectra (EIMS) were recorded on a VG AutoSpec mass spectrometer. Fast atom bombardment mass spectra (FABMS) were recorded on a VG-SAB-SE mass spectrometer. For high resolution FABMS (HRFABMS), the instrument was operated at a resolution of ca. 6000 by employing narrow range voltage scanning along with polyethylene glycol or CsI as reference compounds. <sup>1</sup>H and <sup>13</sup>C NMR spectra were recorded using Bruker AC200 or ARX400 spectrometers with the residual solvent or TMS as the internal standard. The chemical shifts are expressed on the δ scale in parts per million (ppm). The following abbreviations are used for the observed multiplicities: s, singlet; bs, broad singlet; d, doublet; t, triplet; m, multiplet; bm, broad multiplet; dd, double doublet.

**4.1.1. 1,4,7,10,13,20,23,26,29,32-Decaoxa-15,18-diethoxycarbonyl[13,13]paracyclophane (3).** A suspension of **1** (5.0 g, 6.5 mmol), **2** (1.7 g, 6.5 mmol), Cs<sub>2</sub>CO<sub>3</sub> (6.3 g, 19.5 mmol), CsOTs (0.5 g, 2.0 mmol), and KI (0.3 g, 2.0 mmol) in dry MeCN (170 mL) and dry THF (40 mL) was heated at reflux for 1.5 d with continuous stirring. After cooling down to room temperature, the reaction mixture was filtered through celite and the residue was washed with MeCN (200 mL) and CH<sub>2</sub>Cl<sub>2</sub> (100 mL). The solvent was distilled off under reduced pressure and the residue was partitioned between H<sub>2</sub>O (200 mL) and CH<sub>2</sub>Cl<sub>2</sub> (200 mL). The organic layer was washed with brine (150 mL) and the solvent was distilled off under reduced pressure. The residue was purified by column chromatography (SiO<sub>2</sub>, Me<sub>2</sub>CO/hexane 3:2 then Me<sub>2</sub>CO) to give **3** (1.5 g, 34%) as a white solid, mp 84–85°C. FABMS *m/z* 680 [M]<sup>+</sup>; <sup>1</sup>H NMR (200 MHz, CDCl<sub>3</sub>) δ 7.30 (s, 2H), 6.63 (s, 4H), 4.27 (q, *J*=7.1 Hz, 4H), 4.06–4.11 (m, 8H), 3.61–3.98 (m, 24H), 1.27 (t, *J*=7.1 Hz, 6H); <sup>13</sup>C NMR (50 MHz, CDCl<sub>3</sub>) δ 165.4, 153.0, 151.9, 125.1, 117.5, 115.5, 70.9, 70.8, 70.8, 70.7, 70.0, 69.8, 69.6, 68.0, 61.3, 14.3. Anal. calcd for C<sub>34</sub>H<sub>48</sub>O<sub>14</sub>: C, 59.99; H, 7.11. Found: C, 60.34; H, 7.40. Single crystals, suitable for X-ray crystallographic analysis, were grown by slow evaporation of a solution of **3** in heptane and CH<sub>2</sub>Cl<sub>2</sub>. Crystal data: C<sub>34</sub>H<sub>48</sub>O<sub>14</sub>, *M*=680.7, monoclinic, *P*2<sub>1</sub>/*c* (no. 14), *a*=12.232(1), *b*=8.708(1), *c*=32.986(1) Å, β=95.05(1)°, *V*=3499.7(3) Å<sup>3</sup>, *Z*=4, *D*<sub>c</sub>=1.292 g cm<sup>-3</sup>, μ(CuKα)=8.39 cm<sup>-1</sup>, *F*(000)=1456, *T*=293 K; clear prisms, 0.50×0.47×0.33 mm<sup>3</sup>, refined based on *F*<sup>2</sup> to give *R*<sub>1</sub>=0.052, *wR*<sub>2</sub>=0.132 for 3850 independent observed reflections [|*F*<sub>o</sub>|>4σ(*F*<sub>o</sub>)], 2θ≤120° and 450 parameters. CCDC 159795.

**4.1.2. 1,4,7,10,13,20,23,26,29,32-Decaoxa-15,18,34,37-tetra-**

**ethoxycarbonyl[13,13]paracyclophane (5).** A suspension of **2** (8.33 g, 32.8 mmol), **4** (16.66 g, 32.8 mmol), Cs<sub>2</sub>CO<sub>3</sub> (32.00 g, 98.3 mmol), CsOTs (1.00 g, 3.3 mmol), and KI (0.54 g, 3.3 mmol) in dry MeCN (300 mL) and dry THF (50 mL) was heated at reflux for 1.5 d with continuous stirring. After cooling down to room temperature, the reaction mixture was filtered through celite and the residue was washed with MeCN (200 mL) and CH<sub>2</sub>Cl<sub>2</sub> (100 mL). The solvent was distilled off under reduced pressure and the remaining yellow oil was partitioned between H<sub>2</sub>O (200 mL) and CH<sub>2</sub>Cl<sub>2</sub> (200 mL). The organic layer was washed with brine (150 mL) and the solvent was distilled off under reduced pressure. The residue was purified further by column chromatography (SiO<sub>2</sub>, CH<sub>2</sub>Cl<sub>2</sub>/MeOH 100:1 then MeOH) to obtain **5** (3.20 g, 12%) as a white solid, mp 112.8–113.7°C. FABMS *m/z* 825 [M+H]<sup>+</sup>; <sup>1</sup>H NMR (200 MHz, CDCl<sub>3</sub>) δ 7.32 (s, 4H), 4.28 (q, *J*=7.2 Hz, 8H), 4.08–4.13 (m, 8H), 3.79–3.83 (m, 8H), 3.46–3.70 (m, 16H), 1.33 (t, *J*=7.2 Hz, 12H); <sup>13</sup>C NMR (50 MHz, CDCl<sub>3</sub>) δ 165.4, 151.8, 125.0, 117.5, 70.9, 70.8, 70.0, 69.6, 61.2, 14.2. Anal. calcd for C<sub>40</sub>H<sub>56</sub>O<sub>18</sub>: C, 58.24; H, 6.84. Found: C, 58.10; H, 6.45. Single crystals, suitable for X-ray crystallographic analysis, were grown by slow evaporation of a solution of **5** in heptane and CH<sub>2</sub>Cl<sub>2</sub>. Crystal data: C<sub>40</sub>H<sub>56</sub>O<sub>18</sub>·2CH<sub>2</sub>Cl<sub>2</sub>, *M*=994.7, triclinic, *P*1̄ (no. 2), *a*=9.393(2), *b*=9.723(2), *c*=14.483(2) Å, α=103.87(1), β=98.00(2), γ=96.00(2)°, *V*=1258.6(4) Å<sup>3</sup>, *Z*=1 (the molecule has crystallographic *C*<sub>i</sub> symmetry), *D*<sub>c</sub>=1.312 g cm<sup>-3</sup>, μ(CuKα)=27.2 cm<sup>-1</sup>, *F*(000)=524, *T*=293 K; clear blocks, 0.60×0.40×0.20 mm<sup>3</sup>, refined based on *F*<sup>2</sup> to give *R*<sub>1</sub>=0.076, *wR*<sub>2</sub>=0.211 for 2571 independent observed absorption corrected reflections [|*F*<sub>o</sub>|>4σ(*F*<sub>o</sub>)], 2θ≤124° and 299 parameters. CCDC 159796.

**4.1.3. Methyl 5-benzyloxy-2-hydroxybenzoate (7).** To a suspension of K<sub>2</sub>CO<sub>3</sub> (81.6 g, 0.580 mol) in CHCl<sub>3</sub> (800 mL) and MeOH (400 mL), which was maintained at reflux, were added diol **6** (24.5 g, 0.145 mol) and benzyl bromide (17.3 mL, 0.145 mol). The reaction mixture was heated at reflux for an additional 4 h. After cooling down to room temperature, the reaction mixture was filtered and the residue was washed with CHCl<sub>3</sub> (150 mL). The combined organic solution was concentrated under reduced pressure and the residue was dissolved in CHCl<sub>3</sub> (300 mL) and washed with 1 M HCl (2×250 mL). The organic phase was dried (MgSO<sub>4</sub>) and the solvent was distilled off under reduced pressure. The residue was purified by column chromatography (SiO<sub>2</sub>, hexane/AcOEt 6:1) and then recrystallized from a mixture of hexane and CHCl<sub>3</sub> to yield **7** (31.7 g, 85%) as a white solid, mp 110.5–111.3°C. EIMS *m/z* 258 [M]<sup>+</sup>; <sup>1</sup>H NMR (200 MHz, CDCl<sub>3</sub>) δ 10.40 (s, 1H), 7.39–7.46 (m, 5H), 7.36 (d, *J*=2.3 Hz, 1H), 7.15 (dd, *J*=2.3, 9.0 Hz, 1H), 6.93 (d, *J*=9.0 Hz, 1H), 5.02 (s, 2H), 3.95 (s, 3H); <sup>13</sup>C NMR (50 MHz, CDCl<sub>3</sub>) δ 170.3, 156.3, 151.2, 136.9, 128.6, 128.1, 127.6, 124.9, 118.6, 113.6, 112.0, 70.9, 52.4. Anal. calcd for C<sub>15</sub>H<sub>14</sub>O<sub>4</sub>: C, 69.76; H, 5.46. Found: C, 69.73; H, 5.44.

**4.1.4. 1,11-Bis(4'-benzyloxy-2'-methoxycarbonylphenoxy)-3,6,9-trioxaundecane (8).** To a suspension of K<sub>2</sub>CO<sub>3</sub> (12.80 g, 0.092 mol), KI (2.56 g, 0.018 mol), and **7** (20.00 g, 0.077 mol) in MeCN (45 mL), was added a solution of **4** (23.25 g, 0.046 mol) in MeCN (75 mL) at room

temperature. After the addition, the reaction mixture was heated under reflux for 12 h with continuous stirring. After cooling down to room temperature, the reaction mixture was filtered and the solid residue was washed with MeCN (180 mL) and CH<sub>2</sub>Cl<sub>2</sub> (200 mL). The combined organic solution was concentrated under reduced pressure. The residue was dissolved in AcOEt (250 mL) and washed with brine (2×200 mL). The organic phase was dried (MgSO<sub>4</sub>), filtered, and the solvent was distilled off under reduced pressure. Purification of the residue by column chromatography (SiO<sub>2</sub>, CH<sub>2</sub>Cl<sub>2</sub>/MeOH 100:1) yielded **8** (22.8 g, 88%) as a white solid, mp 65.0–65.5°C. EIMS *m/z* 674 [M]<sup>+</sup>; <sup>1</sup>H NMR (200 MHz, CDCl<sub>3</sub>) δ 7.26–7.48 (m, 12H), 7.04 (dd, *J*=3.0, 9.0 Hz, 2H), 6.91 (d, *J*=9.0 Hz, 2H), 4.99 (s, 4H), 4.09–4.21 (m, 4H), 3.85 (s, 6H), 3.62–3.82 (m, 12H); <sup>13</sup>C NMR (50 MHz, CDCl<sub>3</sub>) δ 166.5, 152.9, 152.7, 136.8, 128.6, 128.1, 127.7, 121.6, 120.4, 117.1, 116.6, 71.0, 70.7, 70.7, 70.2, 69.8, 52.1. Anal. calcd for C<sub>38</sub>H<sub>42</sub>O<sub>11</sub>: C, 67.64; H, 6.27. Found: C, 67.32; H, 6.28.

**4.1.5. 1,11-Bis(4'-hydroxy-2'-methoxycarbonylphenoxy)-3,6,9-trioxaundecane (9).** A solution of **8** (8.46 g, 12.6 mmol) in CHCl<sub>3</sub>/MeOH (1:1) (150 mL) was subjected to hydrogenolysis over 10% palladium on activated carbon (6.00 g) and under high pressure of H<sub>2</sub> (30 psi) for 2 d at room temperature. After removal of the catalyst by filtration, the solvent was evaporated to give **9** (6.10 g, >99%) as a pale yellow oil which was employed in the following step without further purification. EIMS *m/z* 494 [M]<sup>+</sup>; <sup>1</sup>H NMR (200 MHz, CD<sub>3</sub>CN) δ 7.15 (d, *J*=2.8 Hz, 2H), 6.99 (dd, *J*=2.8, 8.9 Hz, 2H), 6.85 (d, *J*=8.9 Hz, 2H), 5.77 (bs, 2H), 4.00–4.01 (m, 4H), 3.62–3.73 (m, 12H), 3.68 (s, 6H); <sup>13</sup>C NMR (50 MHz, CD<sub>3</sub>CN) δ 167.5, 152.3, 151.9, 121.9, 121.5, 118.3, 117.4, 71.2, 71.0, 70.7, 70.5, 52.8. Anal. calcd for C<sub>24</sub>H<sub>30</sub>O<sub>11</sub>: C, 58.29; H, 6.12. Found: C, 58.42; H, 6.28.

**4.1.6. 1,4,7,10,13,20,23,26,29,32-Decaoxa-15,35-dimethoxycarbonyl[13,13]paracyclophane (10).** A suspension of **9** (4.3 g, 8.7 mmol), **4** (4.8 g, 9.6 mmol), Cs<sub>2</sub>CO<sub>3</sub> (8.5 g, 26 mmol), CsOTs (0.25 g, 0.87 mmol), and KI (145 mg, 0.87 mmol) in dry MeCN (225 mL) was heated at reflux for 1.5 d with continuous stirring. After cooling down to room temperature, the reaction mixture was filtered through celite and the residue was washed with MeCN (200 mL) and CH<sub>2</sub>Cl<sub>2</sub> (100 mL). The solvent was distilled off under reduced pressure and the yellow oil left was partitioned between H<sub>2</sub>O (200 mL) and CH<sub>2</sub>Cl<sub>2</sub> (200 mL). The organic layer was washed with brine (150 mL) and concentrated under reduced pressure. The residue was purified by column chromatography (SiO<sub>2</sub>, CH<sub>2</sub>Cl<sub>2</sub>/MeOH 40:1) and then recrystallized from a mixture of heptane and CH<sub>2</sub>Cl<sub>2</sub> to give **10** (172 mg, 54%) as a white solid, mp 149°C. FABMS *m/z* 652 [M]<sup>+</sup>; <sup>1</sup>H NMR (200 MHz, CDCl<sub>3</sub>) δ 7.28 (d, *J*=2.9 Hz, 2H), 6.95 (dd, *J*=2.9, 9.0 Hz, 2H), 6.82 (d, *J*=9.0 Hz, 2H), 4.02–4.07 (m, 8H), 3.78–3.93 (m, 8H), 3.83 (s, 6H), 3.65–3.70 (m, 16H); <sup>13</sup>C NMR (50 MHz, CDCl<sub>3</sub>) δ 166.4, 152.9, 152.7, 121.5, 120.4, 116.8, 70.8, 70.3, 69.7, 68.3, 52.0. Anal. calcd for C<sub>32</sub>H<sub>44</sub>O<sub>14</sub>: C, 58.94; H, 6.80. Found: C, 58.62; H, 6.39.

**4.1.7. Complex [10:Na]·PF<sub>6</sub>.** Single crystals of the complex

[**10**:Na]·PF<sub>6</sub>, suitable for X-ray crystallographic analysis, were grown by vapor diffusion of heptane into a Me<sub>2</sub>CO solution of an equimolar mixture of **10** and NaPF<sub>6</sub>. Crystal data: C<sub>32</sub>H<sub>44</sub>O<sub>14</sub>·NaPF<sub>6</sub>·Me<sub>2</sub>CO, *M*=878.7, monoclinic, *P*2<sub>1</sub>/*n* (no. 14), *a*=7.696(1), *b*=20.491(2), *c*=25.574(3) Å, β=91.95(1)°, *V*=4119.0(8) Å<sup>3</sup>, *Z*=4, *D*<sub>c</sub>=1.417 g cm<sup>-3</sup>, μ(CuKα)=15.3 cm<sup>-1</sup>, *F*(000)=1840, *T*=183 K; clear blocky needles, 0.58×0.30×0.17 mm<sup>3</sup>, refined based on *F*<sup>2</sup> to give *R*<sub>1</sub>=0.058, *wR*<sub>2</sub>=0.144 for 4240 independent observed reflections [*I*(*F*<sub>o</sub>)>4σ(*I*(*F*<sub>o</sub>))], 2θ≤120° and 542 parameters. CCDC 159797.

**4.1.8. Complex [3:11]·2PF<sub>6</sub>.** Single crystals of the complex [3:11]·2PF<sub>6</sub>, suitable for X-ray crystallographic analysis, were grown by vapor diffusion of *i*-Pr<sub>2</sub>O into a MeCN solution of an equimolar mixture of **3** and **11**·2PF<sub>6</sub>. Crystal data: C<sub>46</sub>H<sub>62</sub>N<sub>2</sub>O<sub>14</sub>·2PF<sub>6</sub>, *M*=1156.9, monoclinic, *P*2<sub>1</sub>/*c* (no. 14), *a*=14.359(1), *b*=32.866(2), *c*=11.778(1) Å, β=104.93(1)°, *V*=5370.8(5) Å<sup>3</sup>, *Z*=4, *D*<sub>c</sub>=1.431 g cm<sup>-3</sup>, μ(CuKα)=16.8 cm<sup>-1</sup>, *F*(000)=2408, *T*=203 K; red blocks, 0.93×0.50×0.23 mm<sup>3</sup>, refined based on *F*<sup>2</sup> to give *R*<sub>1</sub>=0.076, *wR*<sub>2</sub>=0.195 for 5942 independent observed reflections [*I*(*F*<sub>o</sub>)>4σ(*I*(*F*<sub>o</sub>))], 2θ≤120° and 735 parameters. CCDC 159798.

**4.1.9. 1,4-Bis[2-(2-hydroxyethoxy)ethoxy]-2,5-diethoxycarbonylbenzene (13).** A suspension of **2** (3.0 g, 12 mmol) and K<sub>2</sub>CO<sub>3</sub> (3.6 g, 26 mmol) in dry DMF (35 mL) was stirred for 1 h at room temperature. Then, **12** (3.7 mL, 35 mmol) was added and the temperature was raised to 75°C. Stirring and heating were continued for an additional 2 d. After cooling down to room temperature, the reaction mixture was filtered and the residue was washed with DMF (15 mL). The solvent was distilled off under reduced pressure and the residue was partitioned between CH<sub>2</sub>Cl<sub>2</sub> (150 mL) and H<sub>2</sub>O (70 mL). The pH of the aqueous phase was adjusted to ca. 2 with dilute HCl and then this phase was extracted with CH<sub>2</sub>Cl<sub>2</sub> (2×50 mL). The combined organic solution was washed with H<sub>2</sub>O (80 mL), dried (MgSO<sub>4</sub>), filtered, and concentrated under reduced pressure and the residue was purified by column chromatography (SiO<sub>2</sub>, CH<sub>2</sub>Cl<sub>2</sub>/MeOH 20:1) to afford **13** (0.40 g, 8%) as a colorless oil. HRFABMS calcd for C<sub>20</sub>H<sub>30</sub>O<sub>10</sub>: *m/z* 430.1850. Found: *m/z* 430.1838; <sup>1</sup>H NMR (200 MHz, CD<sub>3</sub>CN) δ 7.35 (s, 2H), 4.30 (q, *J*=7.1 Hz, 4H), 4.31–4.43 (m, 4H), 4.10–4.14 (m, 4H), 3.54–3.80 (m, 8H), 2.63 (s, 2H), 1.30 (t, *J*=7.1 Hz, 6H); <sup>13</sup>C NMR (50 MHz, CDCl<sub>3</sub>) δ 165.4, 152.0, 125.1, 117.6, 72.6, 69.8, 69.5, 61.7, 61.5, 14.3.

**4.1.10. 1,4-Bis[2-(2-hydroxyethoxy)ethoxy]-2-methoxycarbonylbenzene (14).** A suspension of **6** (3.0 g, 18 mmol) and K<sub>2</sub>CO<sub>3</sub> (5.4 g, 39 mmol) in dry DMF (35 mL) was stirred for 1 h at room temperature. Then, **12** (5.6 mL, 54 mmol) was added and the temperature was raised to 75°C. Stirring and heating were continued for an additional 2 d. After cooling down to room temperature, the reaction mixture was filtered and the residue was washed with DMF (15 mL). The solvent was distilled off under reduced pressure and the residue was partitioned between CH<sub>2</sub>Cl<sub>2</sub> (150 mL) and H<sub>2</sub>O (70 mL). The aqueous phase was adjusted to ca. pH 2 with dilute HCl and then this phase was extracted with CH<sub>2</sub>Cl<sub>2</sub> (2×50 mL). Then, the aqueous phase was adjusted to ca. pH 10 with KOH and this phase was



extracted again with  $\text{CH}_2\text{Cl}_2$  (2×50 mL). The combined organic solution was washed with  $\text{H}_2\text{O}$  (80 mL), dried ( $\text{MgSO}_4$ ), filtered, and concentrated under reduced pressure to give **14** (80 mg, 4%) as a yellow oil. HRFABMS calcd for  $\text{C}_{16}\text{H}_{24}\text{O}_8$ :  $m/z$  344.1471. Found:  $m/z$  344.1474;  $^1\text{H}$  NMR (200 MHz,  $\text{CDCl}_3$ )  $\delta$  7.22 (d,  $J=3.0$  Hz, 1H), 6.91 (dd,  $J=3.0, 9.0$  Hz, 1H), 6.81 (d,  $J=9.0$  Hz, 1H), 3.95–4.03 (m, 4H), 3.72 (s, 3H), 3.46–3.74 (m, 12H), 2.76 (s, 2H);  $^1\text{H}$  NMR (400 MHz,  $\text{CD}_3\text{CN}$ )  $\delta$  7.22 (d,  $J=3.0$  Hz, 1H), 7.07 (dd,  $J=3.0, 9.0$  Hz, 1H), 7.02 (d,  $J=9.0$  Hz, 1H), 3.80–4.09 (m, 4H), 3.80 (s, 3H), 3.73–3.76 (m, 4H), 3.53–3.58 (m, 8H);  $^{13}\text{C}$  NMR (50 MHz,  $\text{CDCl}_3$ )  $\delta$  166.2, 152.8, 152.5, 121.2, 120.4, 116.8, 116.2, 72.6, 72.5, 69.8, 69.5, 69.4, 68.1, 61.5, 52.0.

**4.1.11. [2]Catenanes 18-4PF<sub>6</sub>, 19-4PF<sub>6</sub>, and 20-4PF<sub>6</sub>.** A solution of **16-2PF<sub>6</sub>** (70.6 mg, 0.10 mmol), **17** (26.4 mg, 0.10 mmol), and **3**, **5**, or **10** (0.20 mmol) in dry MeCN (6 mL) was stirred for 10 d at room temperature. The solvent was distilled off under reduced pressure and the residue was purified by column chromatography ( $\text{SiO}_2$ , MeOH/2 M  $\text{NH}_4\text{Cl}_{\text{aq}}/\text{MeNO}_2$  7:2:1). The resulting solid was dissolved in  $\text{H}_2\text{O}$  (7 mL) and a saturated aqueous solution of  $\text{NH}_4\text{PF}_6$  was added until no further precipitation occurred. The precipitate was filtered off, washed with  $\text{H}_2\text{O}$  (10 mL), and dried under reduced pressure to afford **18-4PF<sub>6</sub>**, **19-4PF<sub>6</sub>**, or **20-4PF<sub>6</sub>** as a red solid.

**18-4PF<sub>6</sub>** (53%): Mp 298°C (decomposition). FABMS  $m/z$  1635  $[\text{M}-\text{PF}_6]^+$ , 1498  $[\text{M}-2\text{PF}_6]^+$ ;  $^1\text{H}$  NMR (200 MHz,  $\text{CD}_3\text{CN}$ )  $\delta$  8.90 (d,  $J=6.4$  Hz, 8H), 7.80 (s, 8H), 7.65 (d,  $J=6.4$  Hz, 8H), 6.40 (s, 2H), 5.70 (s, 8H), 4.35 (q,  $J=7.0$  Hz, 4H), 3.62–3.94 (m, 36H), 1.40 (t,  $J=7.0$  Hz, 6H);  $^{13}\text{C}$  NMR (50 MHz,  $\text{CDCl}_3$ )  $\delta$  166.5, 151.0, 150.2, 146.4, 145.7, 137.6, 131.8, 126.3, 125.7, 115.3, 113.8, 71.8, 71.1, 70.8, 70.4, 70.3, 69.7, 67.7, 65.7, 62.60, 14.7.

**19-4PF<sub>6</sub>** (3%): Mp 295°C (decomposition). FABMS  $m/z$  1607  $[\text{M}-\text{PF}_6]^+$ , 1462  $[\text{M}-2\text{PF}_6]^+$ , 1317  $[\text{M}-3\text{PF}_6]^+$ ;  $^1\text{H}$  NMR (200 MHz,  $\text{CD}_3\text{CN}$ )  $\delta$  8.92–8.95 (m, 8H), 7.80 (s, 8H), 7.73–7.74 (m, 8H), 7.47–7.57 (m, 2H), 5.71 (bs, 8H), 3.40–3.89 (m, 42H), 1.35–1.41 (m, 12H);  $^{13}\text{C}$  NMR (50 MHz,  $\text{CDCl}_3$ )  $\delta$  166.9, 151.8, 151.8, 151.4, 151.3, 148.0, 146.9, 146.5, 145.8, 140.9, 137.6, 135.2, 133.5, 131.7, 131.2, 130.7, 130.6, 128.4, 126.7, 71.4, 71.2, 71.0, 70.6, 70.4, 68.3, 65.6, 65.2, 64.9, 53.2, 46.1.

**20-4PF<sub>6</sub>** (10%): Mp 301°C (decomposition). FABMS  $m/z$  1463  $[\text{M}-2\text{PF}_6]^+$ , 1317  $[\text{M}-3\text{PF}_6]^+$ , 1172  $[\text{M}-4\text{PF}_6]^+$ ;  $^1\text{H}$  NMR (400 MHz,  $\text{CD}_3\text{CN}$ )  $\delta$  8.92 (bs, 8H), 7.79 (s, 8H), 7.71 (bs, 8H), 6.35 (m, 3H), 5.70 (s, 8H), 3.35–3.95 (m, 41H);  $^{13}\text{C}$  NMR (100 MHz,  $\text{CD}_3\text{CN}$ )  $\delta$  148.7, 146.9, 145.9, 137.65, 131.8, 126.7, 71.5, 71.4, 71.2, 70.4, 65.6. Single crystals of the [2]catenane **20-4PF<sub>6</sub>**, suitable for X-ray crystallographic analysis, were grown by slow evaporation of the compound from a solution in MeCN/ $\text{Et}_2\text{O}$ . Crystal data for **20-4PF<sub>6</sub>**:  $\text{C}_{68}\text{H}_{76}\text{N}_4\text{O}_{14}\cdot 4\text{PF}_6\cdot 3\text{MeCN}$ ,  $M=1876.4$ , triclinic,  $P\bar{1}$  (no. 2),  $a=13.365(2)$ ,  $b=13.810(1)$ ,  $c=26.902(3)$  Å,  $\alpha=87.01(1)$ ,  $\beta=80.87(1)$ ,  $\gamma=61.72(1)^\circ$ ,  $V=4315.6(8)$  Å<sup>3</sup>,  $Z=2$ ,  $D_c=1.444$  g cm<sup>-3</sup>,  $\mu(\text{CuK}\alpha)=18.4$  cm<sup>-1</sup>,  $F(000)=1932$ ,  $T=183$  K; orange/red rhombic needles,  $0.33\times 0.15\times 0.15$  mm<sup>3</sup>, refined based on  $F^2$  to give  $R_1=0.132$ ,  $wR_2=0.344$  for 8122 independent observed

reflections [ $|F_o|>4\sigma(|F_o|)$ ],  $2\theta\leq 120^\circ$ ] and 1201 parameters. CCDC 159799.

## 4.2. Association constants

An equimolar  $\text{CD}_3\text{CN}$  solution of host and guest was diluted from ca.  $10^{-2}$  to ca.  $10^{-3}$  M in 10–15 consecutive steps. The resulting solutions were analyzed by  $^1\text{H}$  NMR spectroscopy at 25°C. The association constants of the complexes were determined<sup>17</sup> by nonlinear curve-fitting of the plot of the chemical shift change associated with the resonance of the  $\beta$ -bipyridinium protons against the concentration.

## References

- (a) Alivastos, A. P.; Barbara, P. F.; Castleman, A. W.; Chang, J.; Dixon, D. A.; Klain, M. L.; Mclendon, G. L.; Miller, J. S.; Ratner, M. A.; Rossky, P. J.; Stupp, S. I.; Thompson, M. E. *Adv. Mater.* **1998**, *10*, 1297–1336. (b) Becker, S.; Müllen, K. In *Stimulating Concepts in Chemistry*; Shibasaki, M., Stoddart, J. F., Vögtle, F., Eds.; Wiley-VCH: Weinheim, 2000; pp 317–337.
- (a) Schill, G. *Catenanes, Rotaxanes, Knots*; Academic: New York, 1971. (b) In *Molecular Catenanes, Rotaxanes, Knots*; Sauvage, J.-P., Dietrich-Buchecker, C. O., Eds.; VCH-Wiley: Weinheim, 1999. (c) Walba, D. M. *Tetrahedron* **1985**, *41*, 3161–3212. (d) Dietrich-Buchecker, C. O.; Sauvage, J.-P. *Chem. Rev.* **1987**, *87*, 795–810. (e) Chambron, J.-C.; Dietrich-Buchecker, C. O.; Sauvage, J.-P. *Top. Curr. Chem.* **1993**, *165*, 131–162. (f) Amabilino, D. B.; Stoddart, J. F. *Chem. Rev.* **1995**, *95*, 2725–2828. (g) Jäger, R.; Vögtle, F. *Angew. Chem., Int. Ed. Engl.* **1997**, *36*, 930–944. (h) Breault, G. A.; Hunter, C. A.; Mayers, P. C. *Tetrahedron* **1999**, *55*, 5265–5293. (i) Seel, C.; Vögtle, F. *Chem. Eur. J.* **2000**, *6*, 21–24.
- (a) Lindsey, J. S. *New J. Chem.* **1991**, *15*, 153–180. (b) Whitesides, G. M.; Mathias, J. P.; Seto, C. T. *Science* **1991**, *254*, 1312–1319. (c) Philp, D.; Stoddart, J. F. *Synlett* **1991**, 445–458. (d) Whitesides, G. M.; Simanek, E. E.; Mathias, J. P.; Seto, C. T.; Chin, D. N.; Mammen, M.; Gordon, D. M. *Acc. Chem. Res.* **1995**, *28*, 37–44. (e) Philp, D.; Stoddart, J. F. *Angew. Chem., Int. Ed. Engl.* **1996**, *35*, 1155–1196. (f) Fyfe, M. C. T.; Stoddart, J. F. *Acc. Chem. Res.* **1997**, *30*, 393–401. (g) Conn, M. M.; Rebek, Jr., J. *Chem. Rev.* **1997**, *97*, 1647–1668. (h) Rebek, Jr., J. *Acc. Chem. Res.* **1999**, *32*, 278–286. (i) Fyfe, M. C. T.; Stoddart, J. F. *Adv. Supramol. Chem.* **1999**, *5*, 1–53. (j) Fyfe, M. C. T.; Stoddart, J. F. *Coord. Chem. Rev.* **1999**, *183*, 139–155.
- (a) *Templated Organic Synthesis*; Diederich, F., Stang, P. J., Eds.; VCH-Wiley: Weinheim, 1999. (b) Busch, D. H.; Stephenson, N. A. *Coord. Chem. Rev.* **1990**, *100*, 119–154. (c) Busch, D. H. *J. Inclusion Phenom.* **1992**, *12*, 389–395. (d) Anderson, S.; Anderson, H. L.; Sanders, J. K. M. *Acc. Chem. Res.* **1993**, *26*, 469–475. (e) Cacciapaglia, R.; Mandolini, L. *Chem. Soc. Rev.* **1993**, *22*, 221–231. (f) Hoss, R.; Vögtle, F. *Angew. Chem., Int. Ed. Engl.* **1994**, *33*, 375–384. (g) Schneider, J. P.; Kelly, J. W. *Chem. Rev.* **1995**, *95*, 2169–2187. (h) Raymo, F. M.; Stoddart, J. F. *Pure Appl. Chem.* **1996**, *68*, 313–322. (i) Hubin, T. J.; Kolchinski, A. G.; Vance, A. L.; Busch, D. L. *Adv. Supramol. Chem.* **1999**, *5*, 237–357. (j) Hubin, T. J.; Busch, D. L. *Coord. Chem. Rev.* **2000**, *200–202*, 5–52.

5. (a) Stoddart, J. F. *Chem. Aust.* **1992**, *59*, 576–577 (see also p 581). (b) Balzani, V. *Tetrahedron* **1992**, *48*, 10443–10514. (c) Preece, J. A.; Stoddart, J. F. *Nanobiology* **1994**, *3*, 149–166. (d) Fabbrizzi, L.; Poggi, A. *Chem. Soc. Rev.* **1995**, *24*, 197–202. (e) Preece, J. A.; Stoddart, J. F. In *Ultimate Limits of Fabrication and Measurements*; Welland, M. E., Gimzewski, J. K., Eds.; Kluwer Academic: Dordrecht, 1996; pp 1–8 (see also pp 225–228). (f) Benniston, A. C. *Chem. Soc. Rev.* **1996**, *25*, 427–435. (g) Gómez-López, M.; Preece, J. A.; Stoddart, J. F. *Nanotechnology* **1996**, *7*, 183–192. (h) Ward, M. D. *Chem. Ind.* **1997**, 640–645. (i) Gómez-López, M.; Stoddart, J. F. *Bull. Soc. Chim. Belg.* **1997**, *106*, 491–500. (j) Beer, P. D. *Acc. Chem. Res.* **1998**, *31*, 71–80. (k) Swager, T. M. *Acc. Chem. Res.* **1998**, *31*, 201–207. (l) Balzani, V.; Gómez-López, M.; Stoddart, J. F. *Acc. Chem. Res.* **1998**, *31*, 405–414. (m) Sauvage, J.-P. *Acc. Chem. Res.* **1998**, *31*, 611–619. (n) Chambron, J.-C.; Sauvage, J.-P. *Chem. Eur. J.* **1998**, *4*, 1362–1366. (o) Niemz, A.; Rotello, V. M. *Acc. Chem. Res.* **1999**, *32*, 42–52. (p) Kaifer, A. E. *Acc. Chem. Res.* **1999**, *32*, 62–71. (q) Fabbrizzi, L.; Licchelli, M.; Pallavicini, P. *Acc. Chem. Res.* **1999**, *32*, 846–853. (r) Leigh, D. A.; Murphy, A. *Chem. Ind.* **1999**, 178–183. (s) Piotrowiak, P. *Chem. Soc. Rev.* **1999**, *28*, 143–150. (t) Blanco, M.-J.; Jiménez, M. C.; Chambron, J.-C.; Heitz, V.; Linke, M.; Sauvage, J.-P. *Chem. Soc. Rev.* **1999**, *28*, 293–305. (u) Balzani, V.; Credi, A.; Venturi, M. In *Supramolecular Science: Where It Is and Where It Is Going*; Ungaro, R., Dalcanele, E., Eds.; Kluwer Academic: Dordrecht, 1999; pp 1–22. (v) Ward, M. D. *Chem. Ind.* **2000**, 22–26. (w) Balzani, V.; Credi, A.; Venturi, M. In *Stimulating Concepts in Chemistry*; Shibasaki, M., Stoddart, J. F., Vögtle, F., Eds.; Wiley-VCH: Weinheim, 2000; pp 255–266. (x) Balzani, V.; Credi, A.; Raymo, F. M.; Stoddart, J. F. *Angew. Chem., Int. Ed.* **2000**, *39*, 3348–3391.
6. (a) Gibson, H. W.; Marand, H. *Adv. Mater.* **1993**, *5*, 11–21. (b) Gibson, H. W.; Bheda, M. C.; Engen, P. T. *Prog. Polym. Sci.* **1994**, *19*, 843–945. (c) Gibson, H. W. In *Large Ring Molecules*; Semlyen, J. A., Ed.; Wiley: New York, 1996; pp 191–202. (d) Raymo, F. M.; Stoddart, J. F. *Chem. Rev.* **1999**, *99*, 1643–1664. (e) Geerts, Y. In *Molecular Catenanes, Rotaxanes, and Knots*; Sauvage, J.-P., Dietrich-Buchecker, C. O., Eds.; VCH-Wiley: Weinheim, 1999; pp 247–276. (f) Raymo, F. M.; Stoddart, J. F. In *Supramolecular Polymerization*; Ciferri, A., Ed.; Dekker: New York, 2000; pp 323–357.
7. (a) Geerts, Y.; Muscat, D.; Müllen, K. *Macromol. Chem. Phys.* **1995**, *196*, 3425–3435. (b) Muscat, D.; Witte, A.; Köhler, W.; Müllen, K.; Geerts, Y. *Macromol. Rapid Commun.* **1997**, *18*, 233–241. (c) Weidmann, J. L.; Kern, J. M.; Sauvage, J.-P.; Geerts, Y.; Muscat, D.; Müllen, K. *Chem. Commun.* **1996**, 1243–1244. (d) Shimada, S.; Ishiwara, K.; Tamaoki, N. *Acta Chem. Scand.* **1998**, *52*, 374–376. (e) Menzer, S.; White, A. J. P.; Williams, D. J.; Belohradsky, M.; Hamers, C.; Raymo, F. M.; Shipway, A. N.; Stoddart, J. F. *Macromolecules* **1998**, *31*, 295–307. (f) Hamers, C.; Raymo, F. M.; Stoddart, J. F. *Eur. J. Org. Chem.* **1998**, 2109–2117. (g) Hamers, C.; Kocian, O.; Raymo, F. M.; Stoddart, J. F. *Adv. Mater.* **1998**, *10*, 1366–1369.
8. Asakawa, M.; Dehaen, G.; L'abbé, G.; Menzer, S.; Nouwen, J.; Raymo, F. M.; Stoddart, J. F.; Williams, D. J. *J. Org. Chem.* **1996**, *61*, 9591–9595.
9. Allwood, B. L.; Spencer, N.; Shahriari-Zavareh, H.; Stoddart, J. F.; Williams, D. J. *J. Chem. Soc., Chem. Commun.* **1987**, 1064–1066.
10. Anelli, P.-L.; Ashton, P. R.; Ballardini, R.; Balzani, V.; Delgado, M.; Gandolfi, M. T.; Goodnow, T. T.; Kaifer, A. E.; Philp, D.; Pietraszkiewicz, M.; Prodi, L.; Reddington, M. V.; Slawin, A. M. Z.; Spencer, N.; Stoddart, J. F.; Vicent, C.; Williams, D. J. *J. Am. Chem. Soc.* **1992**, *114*, 193–218.
11. For a discussion of [C–H···O] hydrogen bonding in bipyridinium-containing molecular and supramolecular assemblies, see: (a) Asakawa, M.; Brown, C. L.; Menzer, S.; Raymo, F. M.; Stoddart, J. F.; Williams, D. J. *J. Am. Chem. Soc.* **1997**, *119*, 2614–2627. (b) Houk, K. N.; Menzer, S.; Newton, S. P.; Raymo, F. M.; Stoddart, J. F.; Williams, D. J. *J. Am. Chem. Soc.* **1999**, *121*, 1479–1487.
12. (a) Raymo, F. M.; Houk, K. N.; Stoddart, J. F. *J. Org. Chem.* **1998**, *63*, 6523–6528. (b) Raymo, F. M.; Houk, K. N.; Stoddart, J. F. *J. Am. Chem. Soc.* **1998**, *120*, 9318–9322. (c) Hansen, J. G.; Feeder, N.; Hamilton, D. G.; Gunter, M. J.; Becher, J.; Sanders, J. K. M. *Org. Lett.* **2000**, *2*, 449–452.
13. Hunter, C. A.; Sanders, J. K. M. *J. Am. Chem. Soc.* **1990**, *112*, 5525–5534.
14. See, for example: (a) Cozzi, F.; Cinquini, M.; Annunziata, R.; Dwyer, T.; Siegel, J. S. *J. Am. Chem. Soc.* **1992**, *114*, 5729–5733. (b) Zhang, J.; Moore, J. S. *J. Am. Chem. Soc.* **1992**, *114*, 9701–9702. (c) Hunter, C. A. *Angew. Chem., Int. Ed. Engl.* **1993**, *32*, 1584–1586. (d) Shetty, A. S.; Zhang, J.; Moore, J. S. *J. Am. Chem. Soc.* **1996**, *118*, 1019–1027.
15. (a) Collier, C. P.; Wong, E. W.; Belohradsky, M.; Raymo, F. M.; Stoddart, J. F.; Kuekes, P. J.; Williams, R. S.; Heath, J. R. *Science* **1999**, *285*, 391–394. (b) Wong, E. W.; Collier, C. P.; Belohradsky, M.; Raymo, F. M.; Stoddart, J. F.; Heath, J. R. *J. Am. Chem. Soc.* **2000**, *122*, 5831–5840. (c) Asakawa, M.; Higuchi, M.; Matternsteig, G.; Nakamura, T.; Pease, A. R.; Raymo, F. M.; Shimizu, T.; Stoddart, J. F. *Adv. Mater.* **2000**, *12*, 1099–1102. (d) Collier, C. P.; Matternsteig, G.; Wong, E. W.; Luo, Y.; Beverly, K.; Sampio, J.; Raymo, F. M.; Stoddart, J. F.; Heath, J. R. *Science* **2000**, *289*, 1172–1175.
16. Perrin, D. D.; Armarego, W. L. F. *Purification of Laboratory Chemicals*; 3rd ed.; Pergamon: Oxford, 1988.
17. Connors, K. A. *Binding Constants*; Wiley: New York, 1987.
18. Ashton, P. R.; Brown, C. L.; Cao, J.; Lee, J. Y.; Newton, S. P.; Raymo, F. M.; Stoddart, J. F.; White, A. J. P.; Williams, D. J. *Eur. J. Org. Chem.* **2001**, 957–965.